Centers for Disease Control and Prevention
STEPHEN B. THACKER
CDC LIBRARY

Interlibrary Loans and Journal Article Requests

Notice Warning Concerning Copyright Restrictions:

The copyright law of the United States (Title 17, United States Code) governs the making of photocopies or other reproductions of copyrighted materials.

Under certain conditions specified in the law, libraries and archives are authorized to furnish a photocopy or other reproduction. One specified condition is that the photocopy or reproduction is not to be *"used for any purpose other than private study, scholarship, or research."* If a user makes a request for, or later uses, a photocopy or reproduction for purposes in excess of "fair use," that user may be liable for copyright infringement.

Upon receipt of this reproduction of the publication you have requested, you understand that the publication may be protected by copyright law. You also understand that you are expected to comply with copyright law and to limit your use to one for private study, scholarship, or research and not to systematically reproduce or in any way make available multiple copies of the publication.

The Stephen B. Thacker CDC Library reserves the right to refuse to accept a copying order if, in its judgment, fulfillment of the order would involve violation of copyright law.

Terms and Conditions for items sent by e-mail:

The contents of the attached document may be protected by copyright law. The CDC copyright policy outlines the responsibilities and guidance related to the reproduction of copyrighted materials at CDC. If the document is protected by copyright law, the following restrictions apply:

- You may print only one paper copy, from which you may not make further copies, except as maybe allowed by law.
- You may not make further electronic copies or convert the file into any other format.
- You may not cut and paste or otherwise alter the text.

5 3 1 9 6 3 7 7

Request # 53196377 **AUG 8, 2023**

Email (PDF) to: docdelivery@cdc.gov

Centers For Disease Control and Prevention (CDC)
Stephen B. Thacker CDC Library
1600 Clifton Road NE
MS H19-1, Bldg 19.
Atlanta, GA 30329-4027

DOCLINE: Copy

Title:	Medical engineering & physics
Title Abbrev:	Med Eng Phys
Citation:	2012 Apr;34(3):386-93. doi: 10.1016/j.medengphy.2011.08.004
Article/Chapter:	An analysis of contact stiffness between a finger and an object when wearing an air-cushioned glove:
Chapter/Article Author(s):	Wu JZ, Wimer BM, Welcome DE, Dong RG
NLM Unique ID:	9422753
PubMed UI:	21890395
ISSN/ISBN:	1350-4533 (Print) 1873-4030 (Electronic)
Fill from:	**Any Format**
NLM Call Number:	W1 ME3101M (Gen)
Publisher:	Butterworth-Heinemann, London :
Copyright:	Copyright Compliance Guidelines
Authorization:	wxo9
Need By:	N/A
Maximum Cost:	**FREE**
Patron Name:	TN: 1378349
Library Groups:	AHSLC, DLVIS, FEDMED, FREESHARE, HHSLC
Phone:	+1 404-639-2772
Fax:	
Email:	docdelivery@cdc.gov
Alt. Delivery:	Article Exchange, Web (PDF)
Latest Route:	**Library**: Life University (GAULFC) **Action**: Received by Lending Library **Via**: Cell 1

Bill to: GAUCDG

Centers For Disease Control and Prevention (CDC)
Stephen B. Thacker CDC Library
1600 Clifton Road NE
MS H19-1, Bldg 19.
Atlanta, GA 30333

Medical Engineering & Physics 34 (2012) 386–393

Contents lists available at ScienceDirect

Medical Engineering & Physics

journal homepage: www.elsevier.com/locate/medengphy

Technical note

An analysis of contact stiffness between a finger and an object when wearing an air-cushioned glove: The effects of the air pressure☆

John Z. Wu*, Bryan M. Wimer, Daniel E. Welcome, Ren G. Dong

National Institute for Occupational Safety and Health, Morgantown, WV, USA

ARTICLE INFO

Article history:
Received 31 March 2011
Received in revised form 5 August 2011
Accepted 9 August 2011

Keywords:
Fingertip
Finite element analysis
Glove
Air-cushioned
Soft tissue mechanics

ABSTRACT

Air-cushioned gloves have the advantages of lighter weight, lower cost, and unique mechanical performance, compared to gloves made of conventional engineering materials. The goal of this study is to analyze the contact interaction between fingers and object when wearing an air-cushioned glove. The contact interactions between the the fingertip and air bubbles, which is considered as a cell of a typical air-cushioned glove, has been analyzed theoretically. Two-dimensional finite element models were developed for the analysis. The fingertip model was assumed to be composed of skin layers, subcutaneous tissue, bone, and nail. The air bubbles were modeled as air sealed in the container of nonelastic membrane. We simulated two common scenarios: a fingertip in contact with one single air bubble and with two air cushion bubbles simultaneously. Our simulation results indicated that the internal air pressure can modulate the fingertip–object contact characteristics. The contact stiffness reaches a minimum when the initial air pressure is equal to 1.3 and 1.05 times of the atmosphere pressure for the single air bubble and the double air bubble contact, respectively. Furthermore, the simulation results indicate that the double air bubble contact will result in smaller volumetric tissue strain than the single air bubble contact for the same force.

Published by Elsevier Ltd on behalf of IPEM.

1. Introduction

Gloves are commonly used as a primary means to protect workers from acute traumatic occupational hand injuries. Epidemiological studies indicated that glove use could help to lower the risk of the injuries associated with lacerations and punctures by 60–70% [13]. However, many other studies showed that workers' performance could be compromised when gloves are used [3], partially due to the increased effort in submaximal tasks and reduced sensitivity [15]. Wearing a work glove was found to contribute to hand-grip fatigue [6]. Lariviere et al.'s [9] study indicated that the surface electromyography (EMG) activity in the forearm, which reflected muscle forces, was related to glove types used. Mital et al. [10] investigated the effects of glove use on muscle loading for operating non-powered hand tools and found that the magnitude of torque exerted on the workpiece varied by glove type. These results were further confirmed by Kinoshita et al. [7], who found that glove thickness and materials, which presumably modify the cutaneous sensation and glove/object friction, influence grip force regulation, and thereby affect the precision handling of small objects. Kovacs et al.'s [8] studies indicated significant differences in the effects of different glove types on the peak force, ratio of peak force to normalized flexor muscle EMG activity, and the ratio of peak force to muscle co-activity. Material stiffness and thickness have been identified as the primary concerns in glove design [11]. All previous studies suggest that there is a need to improve glove design using an ergonomic approach, such that gloves serve not only safety protection means, but also help improve productivity.

The air-cushioned glove is among recent glove products developed for anti-vibration protection. Air bubble cushions have been widely used in cases of the contact interactions between human and equipment, for example, the seat cushion, air bed mattresses, sports shoes, and shock-absorption gloves. In a representative air-cushioned glove, the finger segments are cushioned by separated air bubbles (Fig. 1A). Air cushions have the advantages of light weight, low cost, and unique mechanical performance, compared with other conventional glove materials, such as rubbers and polymers. However, the contact interaction between the finger and air bubbles is not well understood.

One of the most important considerations in ergonomic design of a tool handle is the contact stiffness between the hand and tool handle [4,12,14], i.e., the ratio of the contact force to the local deformations of the contacting bodies. Previous experimental studies

☆ *Disclaimers*: Mention of product and/or company name does not imply endorsement by the National Institute for Occupational Safety and Health. The findings and conclusions in this report are those of the authors and do not necessarily represent the views of the National Institute for Occupational Safety and Health.

* Corresponding author at: NIOSH, 1095 Willowdale Road, Morgantown, WV 26505, USA. Tel.: +1 304 285 5832; fax: +1 304 285 6265.

1350-4533/$ – see front matter. Published by Elsevier Ltd on behalf of IPEM.
doi:10.1016/j.medengphy.2011.08.004

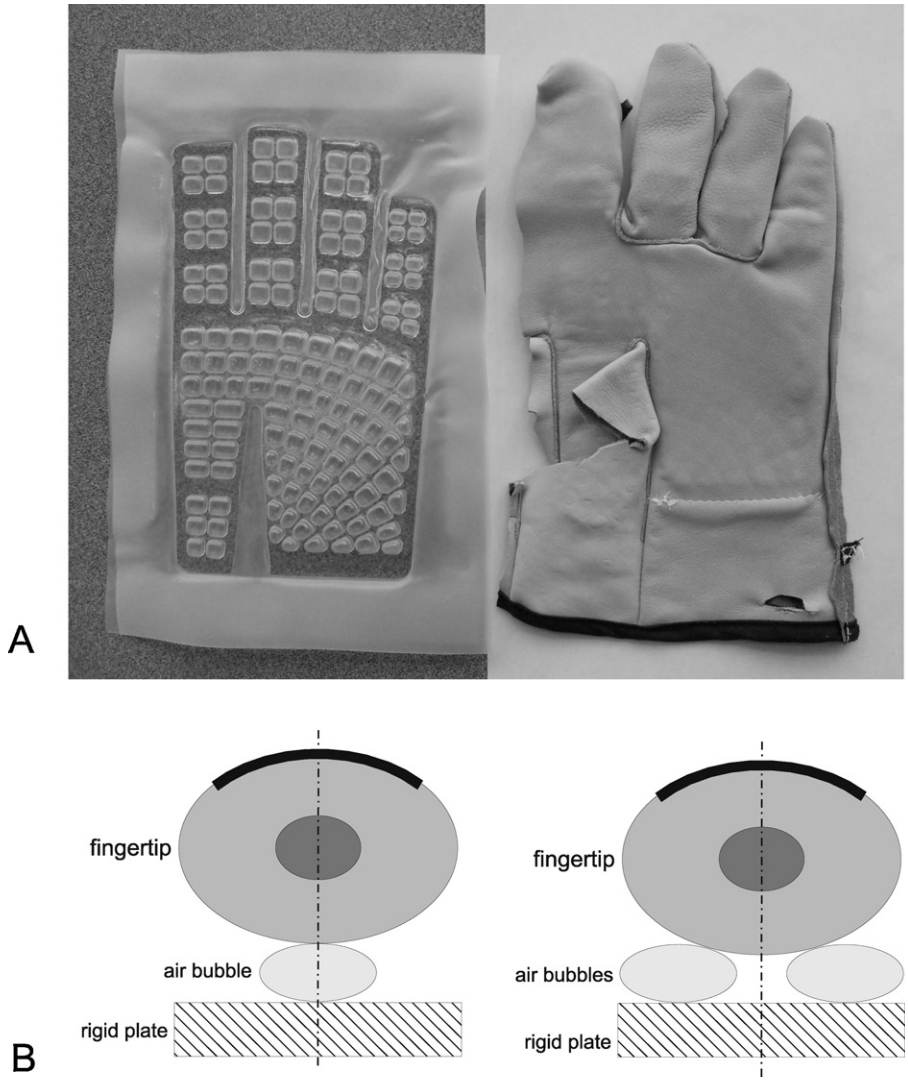

Fig. 1. Illustration of a typical air-cushioned glove and the conceptual models. (A) Typical air-cushioned glove. Left: a piece of air bubble underlay. Right: an air-cushioned glove. (B) Conceptual models. Left: a fingertip contacted with a single air-bubble. Right: a fingertip contacted with two air-bubbles.

indicated that the grip force and the tactile sensitivity of the fingers are effectively affected by the glove thickness [15]. Since glove wearing affects the contact stiffness between the hand and tool handle, these studies suggested that the contact stiffness may affect the manipulations of hand-held tools. The goal of the current study was to analyze the contact interaction between a fingertip and air bubbles, which represents a contact element in an air-cushioned glove. Our hypothesis is that the initial air pressure in the air bubble of the glove will affect the contact stiffness between the fingertip and object.

2. Method

2.1. Finite element models

The mechanical behavior of one cell of a typical air-cushioned glove is analyzed in the current study – the contact interactions between the fingertip and air bubbles. Two scenarios have been simulated, as illustrated in Fig. 1B. In the first case, the fingertip is in contact with a single air bubble (Fig. 1B-left), whereas in the second case, the fingertip is in contact with two air bubbles (Fig. 1B-right) simultaneously. The air-cushion element models are representative for the glove linings that are typically used in mechanic or anti-vibration gloves (e.g., Mechanic, Anti-Vibration Gloves, IMPACTO, Belleville, Canada). The finite element models illustrated in Fig. 2A and B are for these two cases. For the second scenario, only half of the model was considered due to the symmetric nature of the problem (Fig. 1B-right vs. Fig. 2B); the horizontal displacement at the symmetric line was constrained (Fig. 2B). The two-dimensional fingertip model represents a section of the distal finger segment. The section is assumed to be in the middle between the tip of the finger segment and the distal-intermediate phalangeal (DIP) joint line, where the cross-sectional shape variation is considered to be small. The finite element models were developed using a commercial software package COMSOL MultiPhysics (version 3.5a, COMSOL, Inc., Burlington, MA, US).

The fingertip model was assumed to be composed of skin layers, subcutaneous tissue, bone, and nail. The dimensions of the fingertip were assumed to be representative of the index finger of an average male subject [5]. The nail is considered to have a thickness of 0.60 mm [2]. The skin is assumed to be composed of two layers: the outer skin (100 μm thick) and inner skin (1.26 mm thick). The outer skin layer contains stratum corneum (SC) and a part of the viable epidermis; and it is considered as linearly elastic (Young's modulus of 2 MPa and Poisson's ratio of 0.30); whereas the inner skin layer is composed of dermis and a part of the viable epidermis,

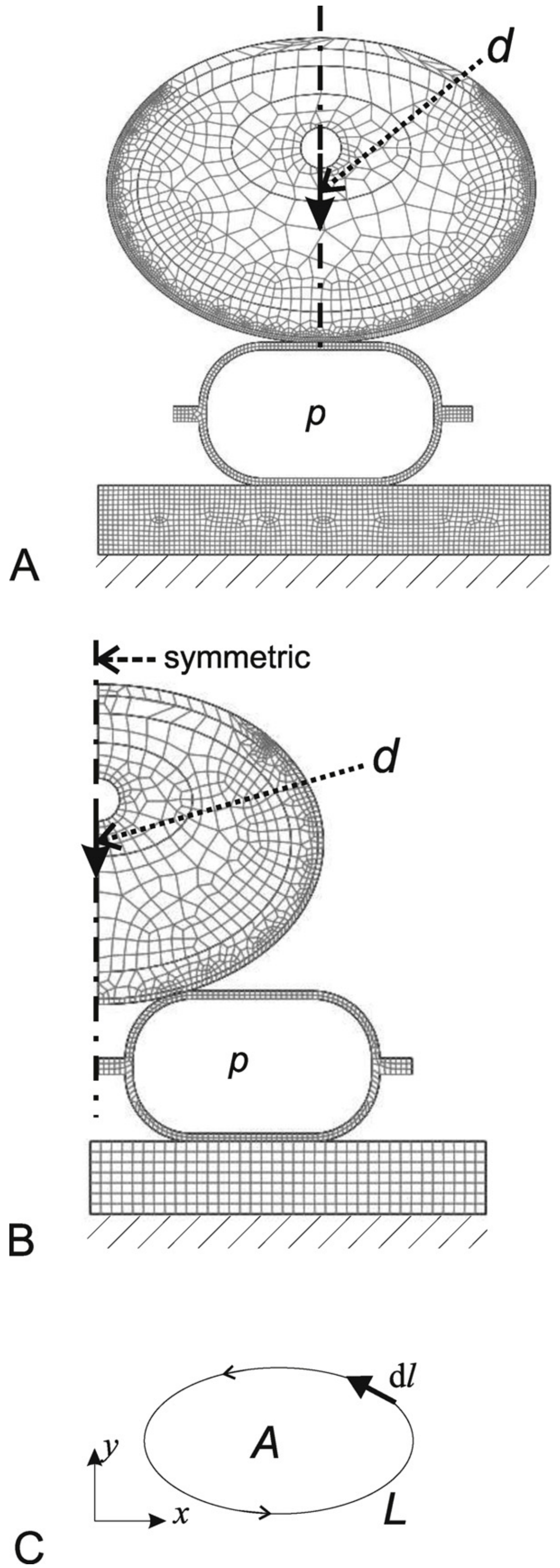

Fig. 2. Finite element models of a fingertip in contact with air bubbles. (A) A fingertip contacted with a single air-bubble cushion. (B) A fingertip contacted with two air-bubble cushions. Only half of the model was considered due to the symmetry. (C) Illustration of the line integration contour. A is the inside area of the air bubble; L is the circumference of A and the domain of the line integration.

and it is characterized as nonlinearly elastic [1]. The bone and nail are assumed to be linearly elastic [18], and have a Poisson's ratio of 0.30 and Young's moduli of 17.0 GPa and 170.0 MPa, respectively. The two-term Mooney–Rivlin model is applied to characterize the nonlinearly elastic behaviors of the subcutaneous tissues and the inner skin layer, as described in our previous studies [16,17].

The membrane of the air bubble has a thickness of 0.3 mm and is made of polyurethane (Stevens Urethane, Easthampton, MA). The mechanical properties of the membrane have been tested via a tensile test (Specimen cross section: 0.34 mm×9.58 mm; specimen gauge length: 30 mm). A micro-mechanical test machine (Model: Mach-1, BioMomentum Inc., Laval, QC, Canada) has been utilized in the material testing. The specimens have been stretched at a very slow rate (0.2 mm/s) in the tests, such that the material's viscous effects are negligible. The obtained stress–strain curves have been fitted to a two-term Mooney–Rivlin model (C10 = 0.1 MPa, C01 = 3.8 MPa).

The base plate was considered to be made of steel with a Young's modulus of 200 GPa and a Poisson's ratio of 0.30.

2.2. Thermodynamics of the air bubble

When an air bubble is compressed, most loading is carried by the internal, compressed air. Since air exhibits a low thermal conductivity, the compression process is considered as isentropic, i.e., the thermal exchange between the air inside the bubble and the surrounding environment is negligible. Thus, the governing equation of the compressed air is expressed as:

$$\frac{p}{p_0} = \left(\frac{V_0}{V}\right)^{\gamma} \tag{1}$$

where p and p_0 are the absolute current and initial pressure, and V and V_0 are the current and the initial bubble volume, respectively; γ is the ratio of the gas specific heat. If we consider the gas within the bubble to be air, $\gamma = 1.4$.

If the initial bubble volume, V_0, is assumed to be the bubble volume at the un-deformed state, correspondingly, the initial pressure is the atmosphere air pressure, $p_0 = p_{at} = 1.01 \times 10^5$ Pa. In the FE modeling, it is more convenient to apply relative pressure inside the air bubble, Δp, which is related to the absolute air pressure (p) by: $p = \Delta p + p_{at}$.

Since the air inside the bubble is considered as a load, and it is not included as a substance in the FE modeling, the direct calculation of air volume from the FE model would not be convenient. Therefore, the volumetric integration of the air is converted into a contour integration on the surface inside the bubble by using Gauss' theorem (Fig. 2C):

$$V = b\int_A \left[\nabla \cdot (x\vec{i} + 0\vec{j})\right] \mathrm{d}a = b\int_A 1\mathrm{d}a = b\oint_L (x\vec{i} + 0\vec{j}) \cdot (\mathrm{d}l_x\vec{i} + \mathrm{d}l_y\vec{j})$$
$$= b\oint_L x\mathrm{d}l_x \tag{2}$$

where ∇ represents the divergence operator; b is the depth of the model, A is the inside cross sectional area, and L is the circumference along the inside membrane; $\vec{i}$ and $\vec{j}$ is the unit vector in the direction of x- and y-axis, respectively; $\mathrm{d}l_x$ and $\mathrm{d}l_y$ is the x- and y-component of the line integration unit $\mathrm{d}l$, respectively.

By combining Eqs. (1) and (2), the relative air pressure applied inside the air bubble, Δp, is expressed as

$$\Delta p = p_{at}\left(\frac{L_0}{\oint_L x\mathrm{d}l_x}\right)^{\gamma} - p_{at} \tag{3}$$

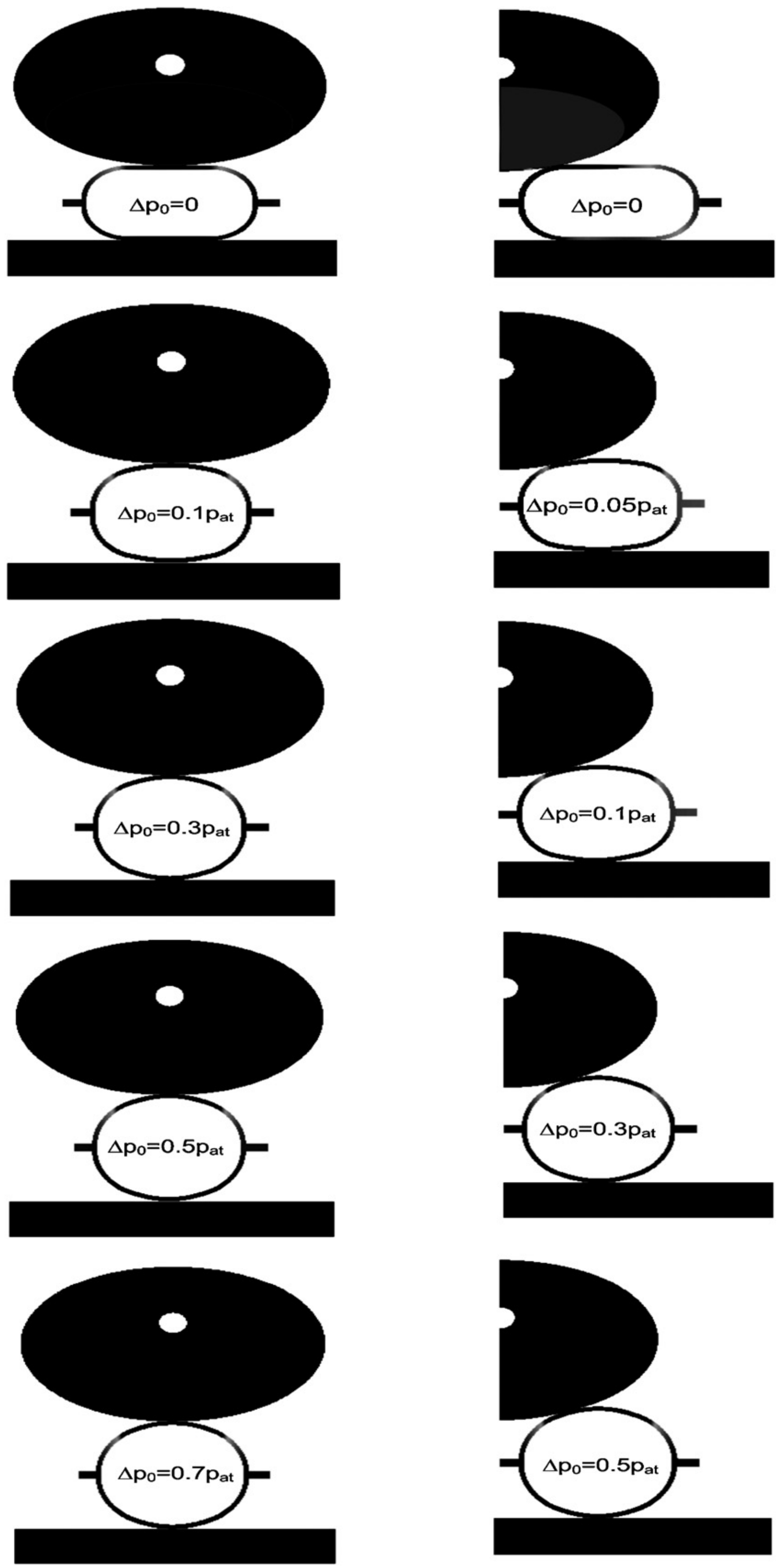

Fig. 3. Deformations of the air bubbles under the initial air. Left column: single air bubble cushion. Right column: double air bubble cushion.

2.3. Numerical simulations

The computations were accomplished in two stages. First, the air bubbles were inflated to the initial volume with the fingertip being held just in contact with the air bubbles (i.e., the contact force was close to zero). Secondly, the fingertip is pressed against the air bubble. The numerical tests for the second stage were performed in a displacement-controlled scheme – the displacement of the fingertip was prescribed at the bone (d) and the contact plate was fixed, whereas the contact force between the air bubble and the fingertip was predicted (Fig. 2).

We simulated two configurations: (1) the fingertip was contacted centrally with one single air bubble (Fig. 2A) and; (2) the fingertip was simultaneously contacted with two air bubbles (Fig. 2B). The initial air pressure, Δp, increased in five stages from 0 to $0.5^* p_{at}$ and $0.7^* p_{at}$, respectively, for the cases of double and single air bubble contact. Δp was treated as a distributed loading that was applied inside the air bubbles, and it was coupled with the deformation of the air bubbles via Eq. (3). We simulated volumetric strains of the tissues and shape variations of the fingertip for different loading conditions. The volumetric strain is defined as the sum of the strains in all three directions. The volumetric strains represent the level of the tissue compression or expansion, whereas the shape variations are represented by the vertical displacements.

3. Results

Before applying air pressure, the air pressure inside and outside of the air bubble is the same (i.e., $\Delta p = 0$). When the air bubbles were inflated to the initial air pressure, the volumes of the air bubbles increased. The predicted deformation and shape variations of the air bubbles as a function of the initial air pressure are shown in Fig. 3. The original shape of the air bubble before being inflated is shown in the plot labeled as $\Delta p = 0$. The fingertip in contact with a single air bubble is shown in the left column; whereas the fingertip in contact with two air bubble is shown in the right column in the figure. Five initial pressure levels were considered for the parametric study: $\Delta p_0/p_{at}$ =0, 0.1, 0.3, 0.5, and 0.7, for the case of single air bubble contact; and $\Delta p_0/p_{at}$ =0, 0.05, 0.1, 0.3, and 0.5, for the case of double air bubble contact. A small force (<0.1 N/m) was applied on the fingertip to establish the initial contact between the fingertip and the air bubble. It is seen that the air bubbles were inflated under the load of the initial internal air pressure.

The predicted contact forces as a function of the displacement for different initial air pressures are shown in Fig. 4. The results for the single air bubble contact are shown in Fig. 4A, whereas those for the double air bubbles contact are shown in Fig. 4B. It is seen that the initial air pressure affects the contact stiffness or the relationship between the contact-force and displacement. The contact stiffness reaches a minimum for certain initial air pressure, i.e., $\Delta p_0/p_{at} = 0.3$ and 0.05, respectively, for the single air bubble and the double air bubble contact.

At the maximal displacement (i.e., 0.003 m as in Fig. 4), the lowermost force–displacement curve reaches a magnitude of 104 N/m (Fig. 4)A, $\Delta p_0/p_{at} = 0.3$). If the same force level (we used here 104 N/m) is applied as a reference, the deformations of the fingertip for different scenarios are comparable. The predicted distributions of the vertical displacement and volumetric strains in the soft tissues of the fingertip at the reference loading magnitude (104 N/m) for the single air bubble contact are shown in left and right column of Fig. 5, respectively. For the same loading (104 N/m), the predicted distributions of the vertical displacement and volumetric strains in the soft tissues of the fingertip for the double air bubble contact are shown in left and right column of Fig. 6, respectively. The results shown are only for two initial air pressures, i.e., the zero relative pressure ($\Delta p_0 = 0$) and the internal air pressure for the minimal contact stiffness. As seen in Fig. 4, the minimal contact stiffness is reached at $\Delta p_0/p_{at} = 0.3$ and 0.05, respectively, for the single air bubble contact and double air bubble contact. The maximal displacements were observed at the contact interface between the air bubble and fingertip skin surface. The maximal volumetric strains in the soft tissues were found at the bone–tissue interface and within the subcutaneous tissue.

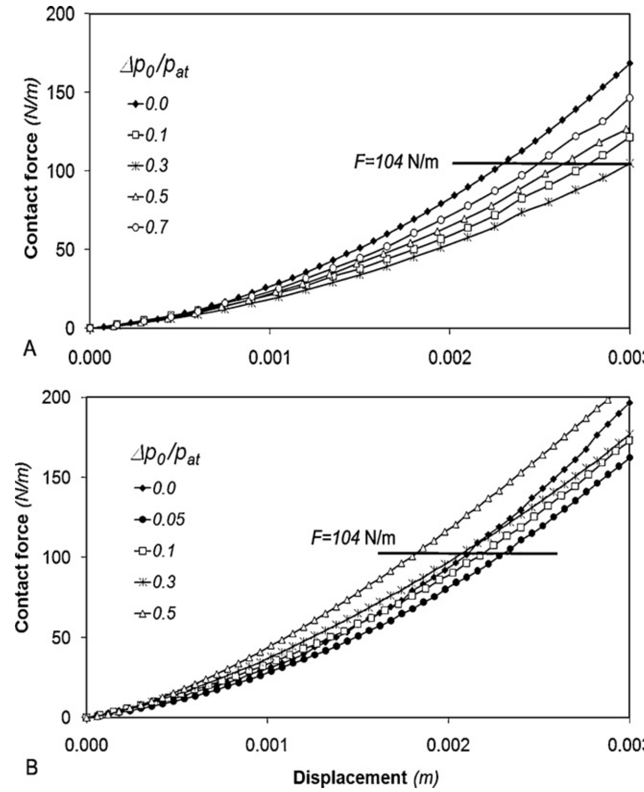

Fig. 4. The relationship between the contact force and displacement when the fingertip compressed against air bubbles. (A) Single air bubble cushion. (B) Double air bubble cushion.

4. Discussion and conclusion

The simulations were performed in a quasi-static manner in the current study. The effects of the mass on the tissues stress/strain distribution and contact stiffness were not considered. In the operation of non-powered tools for most maintenance and construction jobs, the effects of the mass on the mechanical responses of the fingertip are negligible. However, the air-cushioned gloves are also applied in anti-vibration protections, in which the mass effects will play a predominant role. These issues are beyond the scope of the current study.

Our simulations indicated that the relationship between the initial air pressure and the contact stiffness is highly nonlinear. The contact stiffness is dependent on the air pressure, the shape of the inflated air bubble, and the tissue deformation of the finger. When the fingers are pressed on an object with increasing contact force, the air bubbles are compressed and their volumes are decreased, resulting in an increase of the air pressure inside the bubble. The increase of the air pressure will cause the increase of the stretch in the membrane of the air bubbles, enlarging the volume of the air bubbles, which in turn decreases the air pressure. In addition, the air bubbles become flattened under compressive loading, increasing the contact area and, thereby, varying the contact pressure distributions. Finally, the contact force, contact pressure, air pressure, and shape and volume variations of the air bubbles will reach an equilibrium. The initial air pressure in the bubbles is thus nonlinearly coupled with the contact force.

Our simulations indicated that the initial air pressure affects the contact interaction for the single air cushion contact differently than that for the double air cushion contact. In a typical air-cushion glove, fingers may be in contact with two air bubbles simultaneously in most places, but they may also contact with a single air bubble in some locations. The present findings indicate that the

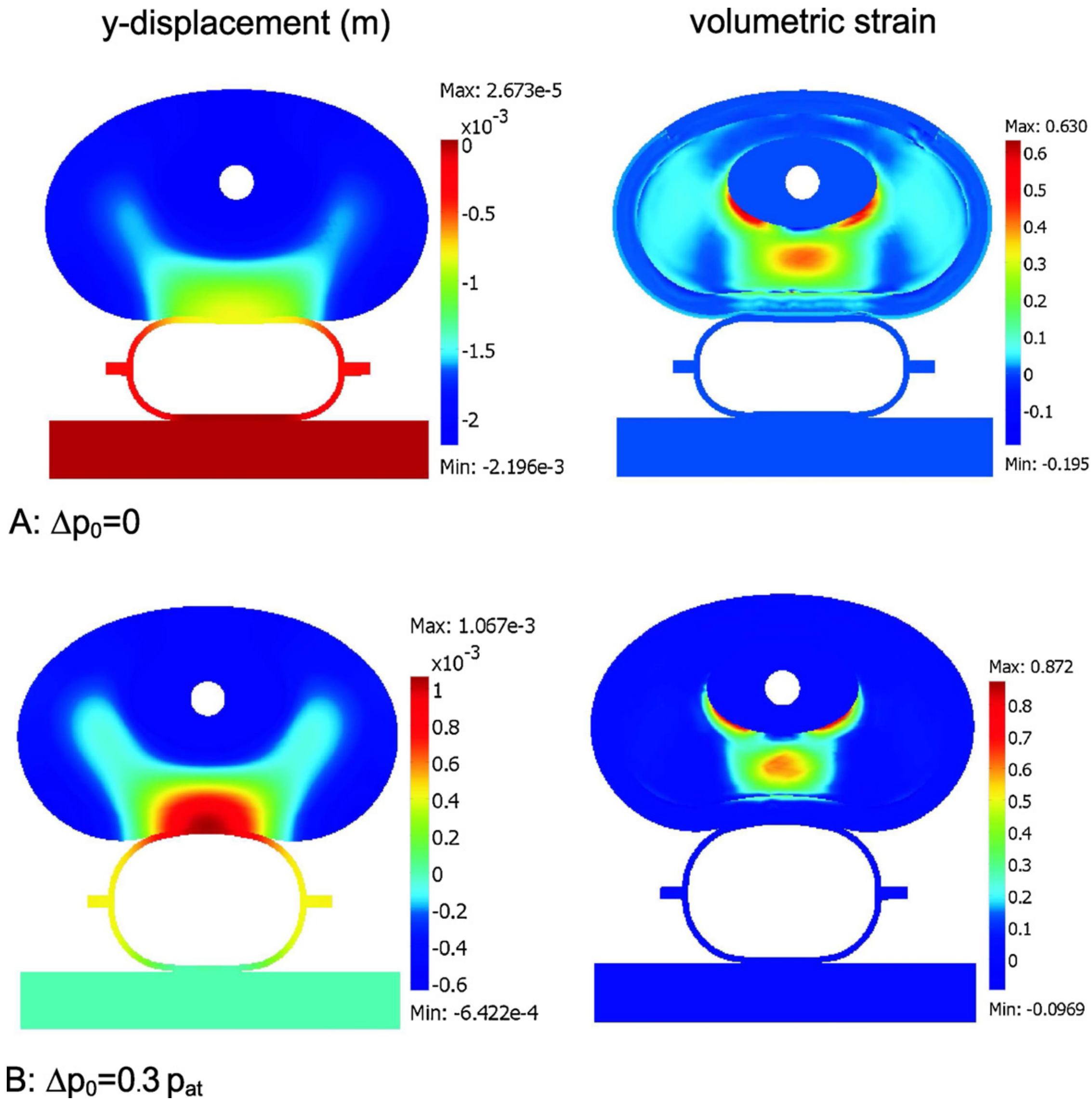

Fig. 5. Deformation of the fingertip and air bubble at F = 104 N/m (as shown in Fig. 4A) predicted using the single air-bubble cushion model. Left: vertical displacement. Right: volumetric strain. Two initial air pressures, $\Delta p_0 = 0$ and $\Delta p_0 = 0.3\,p_{at}$, were considered.

air bubbles should be inflated to different initial air pressures for the single- and double air-cushion contact to achieve an optimized performance in terms of the contact stiffness.

Both numerical tests of the single and double air bubble contact showed that there are two maximums of the volumetric strain in the soft tissues: one is close to the bone–tissue interface and one is within the subcutaneous tissue. In the current model, the material properties vary suddenly from the stiff bone to the relatively soft subcutaneous tissue in the bone–tissue interface. In physiological conditions, the material properties of the bone and subcutaneous tissue are not homogeneous and isotropic; and there exists a transition in the material properties in the bone–tissue interface, which is not considered in the current FE modeling. Therefore, the predicted strains in the bone–tissue interface may contain artifacts due to the simplifying assumption in the FE modeling.

It is interesting to see that the location of the maximal volumetric strain for the single air bubble contact is approximately at the center of the subcutaneous tissues (Fig. 5B), whereas the maximal volumetric strain for the double air bubble contact is close to the skin–subcutaneous conjunction (Fig. 6B). These results imply that, when applying a great compressive force on the air bubbles, one might feel discomfort at the deep tissue level of the fingertip for a single air bubble contact, whereas one might feel discomfort near the skin surface for double air bubble contact.

Our simulation results show that, for the same contact force (104 N/m), the volumetric strain in the soft tissues for double air bubble contact is approximately 50% of that for the single air bubble contact. These results imply that, when applying the same compressive force, the operator may feel more comfort wearing a glove with mostly double air bubble cushion than wearing a glove with mostly the single air bubble cushion.

For the scenario of a single air bubble contact, the maximal volumetric strain in the soft tissues for $\Delta p_0 = 0$ is approximately 50% of that at $\Delta p_0/p_{at} = 0.3$ (i.e., the air pressure at minimized contact stiffness, as Fig. 5). However, for the double air-cushioned contact, the maximal volumetric strain in the soft tissues for $\Delta p_0 = 0$ is about identical to that at the minimized contact stiffness ($\Delta p_0/p_{at} = 0.05$, as Fig. 6). These simulation results further suggest that the double air-cushion contact will result in the minimal volumetric tissue strain.

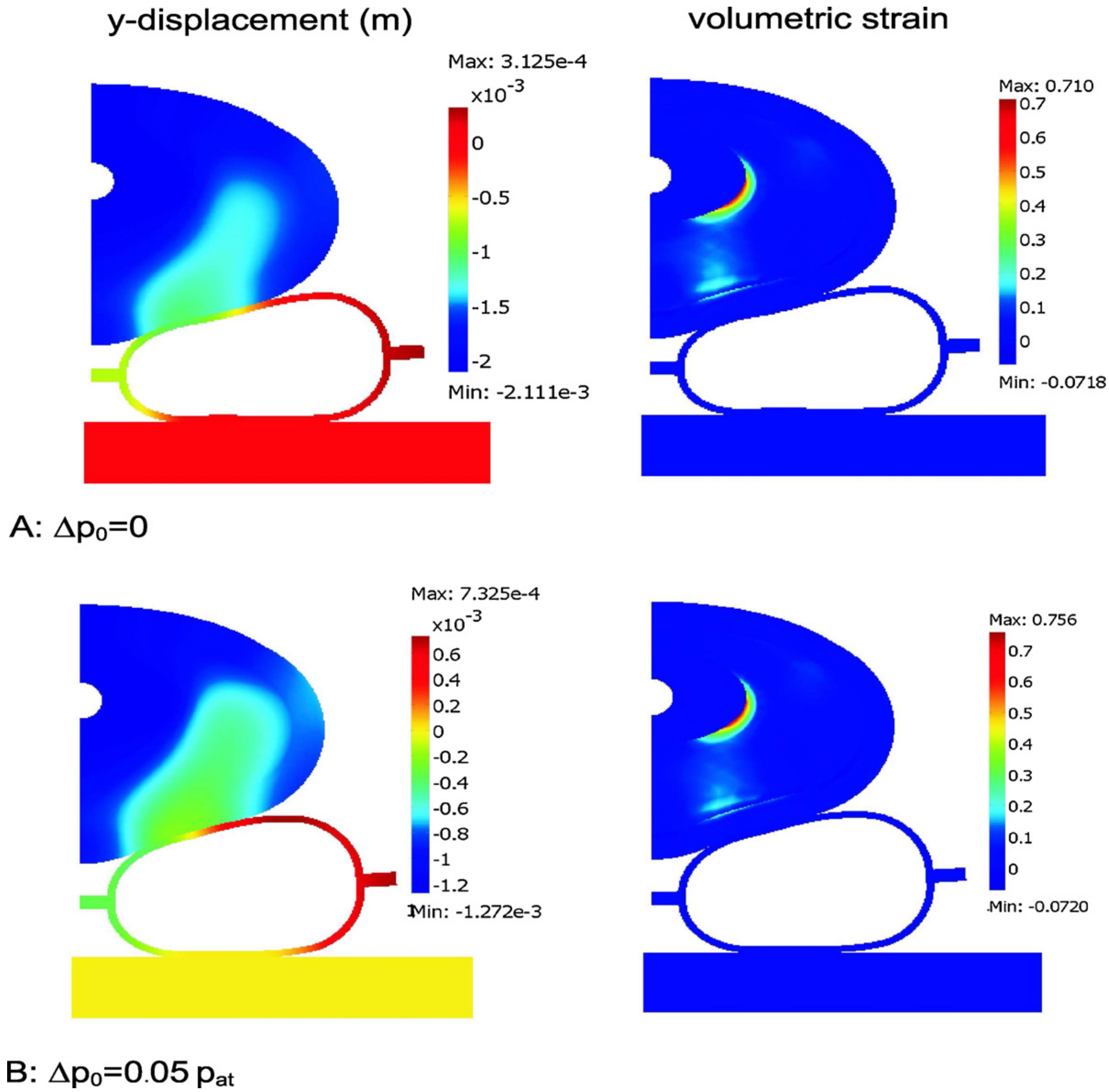

Fig. 6. Deformation of the fingertip and air bubble at $F = 104$ N/m (as shown in Fig. 4B) predicted using the double air-bubble cushion model. Left: vertical displacement. Right: volumetric strain. Two initial air pressures, $\Delta p_0 = 0$ and $\Delta p_0 = 0.05\, p_{at}$, were considered.

Acknowledgements

We want to express our gratitude to Dr. Robert G. Cutlip and Mr. James S. Ensey (NIOSH), who measured the mechanical properties of the air bubble materials. We would also like to thank IMPACTO (Belleville, Canada), who provided the study with samples of air-cushioned gloves.

Conflict of interest

The authors declare that there is no conflict of interest.

References

[1] Agache PG, Monneur C, Leveque JL, De Rigal J. Mechanical properties and Young's modulus of human skin in vivo. Arch Dermatol Res 1980;269(3):221–32.
[2] Baran R. Nail anatomy and physiology. In: Agache P, Humbert P, editors. Measuring the skin. Berlin, Heidelberg: Springer-Verlag; 2004. p. 290–3.
[3] Bishu RR, Kim B, Klute G. Force-endurance relationship: does it matter if gloves are donned? Appl Ergon 1995;26(3):179–85.
[4] Bobjer O, Johansson SE, Piguet S. Friction between hand and handle. effects of oil and lard on textured and non-textured surfaces; perception of discomfort. Appl Ergon 1993;24(3):190–202.
[5] Clemente C. In: Anatomy: a regional atlas of the human body. 2nd edition Baltimore-Munich: Urban and Achwarzengerg; 1981.
[6] Fleming SL, Jansen CW, Hasson SM. Effect of work glove and type of muscle action on grip fatigue. Ergonomics 1997;40(6):601–12.
[7] Kinoshita H. Effect of gloves on prehensile forces during lifting and holding tasks. Ergonomics 1999;42(10):1372–85.
[8] Kovacs K, Splittstoesser R, Maronitis A, Marras WS. Grip force and muscle activity differences due to glove type. AIHA J (Fairfax, Va) 2002;63(3):269–74.
[9] Lariviere C, Tremblay G, Nadeau S, Harrabi L, Dolez P, Vu-Khanh T, et al. Do mechanical tests of glove stiffness provide relevant information relative to their effects on the musculoskeletal system? A comparison with surface electromyography and psychophysical methods. Appl Ergon 2010;41(2):326–34.
[10] Mital A, Kuo T, Faard HF. A quantitative evaluation of gloves used with non-powered hand tools in routine maintenance tasks. Ergonomics 1994;37(2):333–43.
[11] Muralidhar A, Bishu RR, Hallbeck MS. The development and evaluation of an ergonomic glove. Appl Ergon 1999;30(6):555–63.
[12] Seo NJ, Armstrong TJ. Investigation of grip force, normal force, contact area, hand size, and handle size for cylindrical handles. Hum Factors 2008;50(5):734–44.
[13] Sorock GS, Lombardi DA, Peng DK, Hauser R, Eisen EA, Herrick RF, et al. Glove use and the relative risk of acute hand injury: a case-crossover study. J Occup Environ Hyg 2004;1(3):182–90.
[14] van Veelen MA, Meijer DW, Goossens RH, Snijders CJ. New ergonomic design criteria for handles of laparoscopic dissection forceps. J Laparoendosc Adv Surg Tech A 2001;11(1):17–26.

[15] Willms K, Wells R, Carnahan H. Glove attributes and their contribution to force decrement and increased effort in power grip. Hum Factors 2009;51(6):797–812.
[16] Wu JZ, Dong RG, Welcome DE. Analysis of the point mechanical impedance of fingerpad in vibration. Med Eng Phys 2006;28(8):816–26.
[17] Wu JZ, Welcome DE, Dong RG. Three-dimensional finite element simulations of the mechanical response of the fingertip to static and dynamic compressions. Comput Methods Biomech Biomed Engin 2006;9(1):55–63.
[18] Yamada H. In: Strength of biological materials. Baltimore: Williams and Wilkins Co; 1970.